Theoretical Compton profiles of graphite and LiC_6

M. Y. Chou, Marvin L. Cohen, and Steven G. Louie
Department of Physics, University of California, and Materials and Molecular Research Division, Lawrence Berkeley Laboratory, Berkeley, California 94720
(Received 24 December 1985)

Within the impulse approximation, Compton profiles of graphite and LiC_6 for several symmetry directions are calculated using the wave functions obtained from pseudopotential local-density-functional calculations. Excellent agreement is found when the calculated profiles are compared with the experimental results. The intercalation effects were analyzed in the difference profile between these two materials.

I. INTRODUCTION

The properties of graphite and graphite intercalation compounds (GIC's) have been the subject of many theoretical and experimental studies in recent years.[1,2] Graphite itself is a prototype quasi-two-dimensional material. It consists of layers of atoms with stacking sequence $ABAB\cdots$. Within a layer, the carbon atoms form a hexagonal lattice with very strong bonding between them. The interlayer interaction is relatively weak, which makes it possible to diffuse foreign atoms or molecules into the space between carbon layers. Many physical properties are dramatically changed upon intercalation.[2] They are both physically and chemically interesting and offer a wide range of possible technological applications.

In this study, we will concentrate on a first-stage graphite intercalation compound, LiC_6. Upon intercalation, the stacking sequence of the carbon layers is changed to $A\alpha A\alpha\cdots$, where α stands for lithium atoms which exist between every single carbon layer. There is a 10% expansion of the interlayer distance in LiC_6 and the conductivity anisotropy is largely reduced.[2] The ratio of the electrical conductivity in the basal plane relative to its value perpendicular to the plane is reduced from about 10^3 in graphite to 10^1 in LiC_6. Because the crystal structure is simple (six carbon atoms and one lithium atom per unit cell), realistic band-structure calculations have become feasible.[3–5] It is believed from the band-structure calculations that lithium acts as an electron donor in this system. The previously empty π^* (antibonding) orbitals in graphite are partially filled by the excess $2s$ electrons from the lithium atoms and the Fermi level is raised accordingly. This is the so-called rigid-band model. It is also found experimentally that the band states with dominant s character of the intercalant (in this case lithium $2s$) are above the Fermi level and are unoccupied.[6–8]

There are several independent experiments which support, directly or indirectly, this charge transfer picture. The binding energy of the lithium $1s$ state in LiC_6 is found to be much closer to its value in LiF than that in lithium metal.[7,9] This indicates that lithium in LiC_6 resembles a Li^+ ion. When the unoccupied states on different sites are probed selectively by photoelectric yield measurements on LiC_6 and graphite,[10] it is found that the electronic states in the vicinity of Fermi level in LiC_6 are mainly carbon orbitals with π symmetry. The experimental ^7Li quadrupole coupling constant in LiC_6 is consistent with that derived from a simple model, in which the average locations of the electrons transferred from the lithium intercalant are taken to be the spatial charge distribution of the π-type orbitals.[11] Moreover, a study of the ^{13}C NMR peak in LiC_6 reveals a shift towards high field compared with that in graphite.[12] This effect was attributed to an indirect Knight shift resulting from the polarization of core s electrons by the delocalized conduction π electrons and from the enhancement of the density of states at the Fermi level in LiC_6.

Although the rigid-band model works well in explaining qualitatively many experimental properties, the lithium intercalant does interact with graphite, resulting in modification of the electronic energy bands. As is observed in the angle-resolved photoemission experiment on LiC_6 and graphite[7], the valence bands do not shift uniformly upon intercalation. Self-consistent pseudopotential calculations have been performed for graphite and LiC_6.[5,13] The calculated electronic bands of graphite and LiC_6 are similar when the graphite energy bands are folded into the same Brillouin zone, yet there exist appreciable differences. These differences are related to the intercalant host interactions and the change in the stacking sequence.

Within the impulse approximation,[14] the Compton scattering (electron-photon scattering) profiles can be used to determine the electron momentum distribution of the system along selected directions.[15] It was suggested forty years ago[16] that this could help in understanding carbon bonds in different molecules. Subsequent measurements have been successful in identifying a particular profile with a particular carbon bond for a series of molecular hydrocarbons.[17] When applied to solids, these measurements also serve as a sensitive test of the ground-state wave functions. The Compton profiles for graphite have been measured by several groups[18–23] and, more recently, for LiC_6.[21] In this work, we calculate the Compton profiles of graphite and LiC_6 along several directions using the wave functions obtained from previous self-consistent band-structure studies,[5,13] and compare them with some

recent experimental results. Part of the results have been briefly reported previously.[24] In order to examine the effects resulting from the change of the stacking pattern and the increase of the interlayer distance, the Compton profile is also calculated for an artificial crystal C_6 which has the identical structure of LiC_6 but with the lithium atoms removed. This study should provide an alternative point of view by considering the effects of intercalation on momentum space properties. The agreement between the calculated and measured profiles of graphite and LiC_6 is excellent, especially for the profile anisotropy. From the difference between profiles of LiC_6 and graphite, one can observe the effect of polarization induced by the intercalant and several special features arising from the conduction bands of LiC_6.

The rest of this paper is organized as follows; the calculational details are presented in Sec. II, the calculated results and comparison with experiments are in Sec. III, and conclusions are given in Sec. IV.

II. CALCULATIONS

The cross section for Compton scattering from bound electrons in solids is too complex to be evaluated exactly. Usually, an impulse approximation[14] is used in which the electronic potential is assumed constant during the short time of scattering. This leads to a final expression which treats the initial electron with momentum p_i as having energy $p_i^2/2m$ measured from the instantaneous constant potential. The resulting spectrum of the scattered photons is then directly related to the electron momentum distribution in this system projected along the scattering-vector direction. This approximation is valid when the electron recoil energy is much larger than the binding energy and the scattering involves a single electron. It is an appropriate assumption when incoming photons are in the region of x rays or γ rays.

Using this impulse approximation, the expression for the Compton profile along a specific direction $\hat{\mathbf{e}}$ is

$$J(q,\hat{\mathbf{e}})=\frac{1}{N}\sum_{n}\sum_{\mathbf{k}}\sum_{\mathbf{G}}|C_{n,\mathbf{k}}(\mathbf{G})|^2\Theta(E_F-E_{n,\mathbf{k}}) \times\delta((\mathbf{k}+\mathbf{G})\cdot\hat{\mathbf{e}}-q)\,, \quad (1)$$

where n represents the band index, E_F is the Fermi energy, and $C_{n,\mathbf{k}}(\mathbf{G})$ is the coefficient of the plane wave $e^{i(\mathbf{k}+\mathbf{G})\cdot\mathbf{r}}$ for the plane-wave expansion of the wave function $\Psi_{n,\mathbf{k}}(\mathbf{r})$ corresponding to energy $E_{n,\mathbf{k}}$. The summation over $\mathbf{G}$ is straightforward and includes about 600 and 1000 reciprocal-lattice vectors for graphite and LiC_6, respectively. The summation over the k points is carried out by the tetrahedral linear interpolation method.[25] A grid of 45 k points in the irreducible zone is used which corresponds to three grid points from Γ to A and five grid points from Γ to M or K.

The band-structure calculations were performed using the pseudopotential technique[26] and the local-density-functional approximation.[27] A mixed basis set which consists of plane waves and linear combinations of atomic orbitals[28] is used to represent the wave functions. The results for the occupied bands in graphite[13] are in good agreement with other calculations[29] and with angle-resolved photoemission experiment.[7] Because of the use of pseudopotentials, the core electrons are not included in this calculation. In addition, the pseudo-wave-functions do not have oscillations near the nuclei; therefore the amplitude of the calculated Compton profile at large momenta is expected to be smaller than that of an all-electron calculation.

In LiC_6, the lithium atoms are located in the center positions between two carbon hexagons and form a $\sqrt{3}\times\sqrt{3}$ lattice compared with the in-plane lattice vectors of graphite. The intralayer and interlayer dilations are about 1% and 10%, respectively, upon intercalation. A tabulation of the structural information can be found in Ref. 5. In order to make consistent comparisons, the crystal C_6 is calculated in the same unit cell as LiC_6. Using the wave functions of graphite, C_6, and LiC_6, the Compton profiles are computed for the symmetry directions of [0001], [11$\bar{2}$0], and [10$\bar{1}$0]. Since the xy-plane lattice vectors in the plane for graphite and LiC_6 make an angle of 30°, the Brillouin-zone projections shown in Fig. 1 have different orientations relative to the hexagonal rings of carbon atoms in the real space. As a result, the Γ-to-M direction in graphite corresponds to the Γ-to-K direction in LiC_6 and *vice versa*. Hence the graphite [10$\bar{1}$0] ([11$\bar{2}$0]) profile should be compared with the LiC_6 [11$\bar{2}$0] ([10$\bar{1}$0]) profile.

In the measurements of Compton scattering for graphite, highly oriented pyrolytic graphite (HOPG) is often used as the sample. The c axis is highly oriented but the xy direction is completely random. As a result the experiment measures profiles along the c axis and those averaged over the xy plane. In our calculation, the averaged profile over the xy plane is obtained by taking the average of those along eight even spaced directions in one irreducible Brillouin zone.

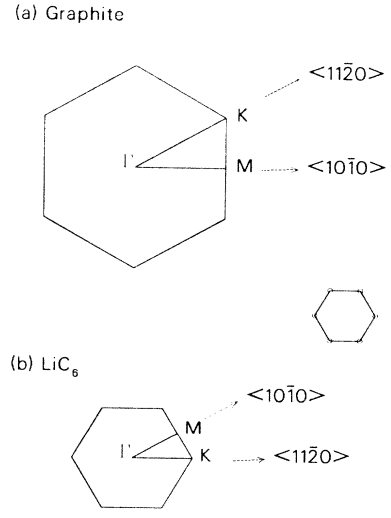

FIG. 1. The first Brillouin zone projected on the xy plane for (a) graphite and (b) LiC_6. The relative orientation with respect to the hexagonal carbon ring in real space is shown.

III. RESULTS AND DISCUSSIONS

A. Calculated results

Tables I and II list the calculated profiles along several directions for graphite and LiC_6, respectively. The profile is normalized in such a way that, when integrated from $-\infty$ to $+\infty$, it gives 4 for graphite or $4\frac{1}{6}$ for LiC_6. These are the average numbers of electrons per carbon atom. The Rydberg unit is used for the momentum where $e^2=2$, $m_e=\frac{1}{2}$, and $h/2\pi=1$.

The calculated profiles of graphite (solid line) and LiC_6 (dashed line) along the [0001] direction (the c axis) are plotted in Fig. 2. Because the average numbers of electrons per carbon atom are not the same, the LiC_6 profile has a slightly higher amplitude mostly concentrating at momenta less than 0.8 a.u. The apparent noise in the curves results from the use of a finite number of k points in the linear interpolation in the tetrahedral integration method.

In order to examine the differences between the curves in Fig. 2 more closely, the contribution from various energy bands are shown in Fig. 3. We divide the profile into three parts: contributions from the occupied σ bands

TABLE I. Calculated valence-electron Compton profiles along several symmetry directions for graphite.

q	[0001]	[10$\bar{1}$0]	[11$\bar{2}$0]	xy
0.0	1.938	1.959	2.009	1.988
0.1	1.933	1.961	1.997	1.978
0.2	1.915	1.931	1.972	1.949
0.3	1.877	1.876	1.926	1.899
0.4	1.818	1.816	1.834	1.826
0.5	1.732	1.739	1.704	1.727
0.6	1.604	1.644	1.552	1.596
0.7	1.443	1.477	1.380	1.425
0.8	1.270	1.282	1.213	1.244
0.9	1.067	1.068	1.058	1.064
1.0	0.863	0.887	0.912	0.903
1.1	0.686	0.749	0.803	0.780
1.2	0.550	0.610	0.683	0.647
1.3	0.439	0.480	0.530	0.505
1.4	0.358	0.362	0.375	0.367
1.5	0.290	0.265	0.242	0.253
1.6	0.232	0.196	0.159	0.175
1.7	0.182	0.143	0.110	0.124
1.8	0.145	0.103	0.083	0.091
1.9	0.114	0.076	0.065	0.069
2.0	0.091	0.055	0.052	0.054
2.2	0.060	0.031	0.035	0.034
2.4	0.039	0.020	0.027	0.025
2.6	0.027	0.017	0.025	0.020
2.8	0.020	0.015	0.022	0.017
3.0	0.014	0.014	0.015	0.015
3.2	0.010	0.013	0.011	0.012
3.4	0.007	0.011	0.007	0.009
3.6	0.005	0.009	0.005	0.007
3.8	0.003	0.006	0.004	0.005
4.0	0.002	0.004	0.004	0.004

TABLE II. Calculated valence-electron Compton profiles along several symmetry directions for LiC_6.

q	[0001]	[11$\bar{2}$0]	[10$\bar{1}$0]	xy
0.0	2.000	2.149	2.066	2.073
0.1	1.999	2.085	2.058	2.064
0.2	2.009	2.001	2.034	2.035
0.3	1.979	1.939	1.999	1.986
0.4	1.938	1.872	1.946	1.915
0.5	1.854	1.798	1.867	1.820
0.6	1.720	1.707	1.708	1.696
0.7	1.546	1.594	1.467	1.543
0.8	1.296	1.445	1.283	1.352
0.9	1.073	1.123	1.108	1.113
1.0	0.875	0.911	0.954	0.939
1.1	0.684	0.753	0.820	0.793
1.2	0.558	0.609	0.685	0.648
1.3	0.449	0.475	0.521	0.498
1.4	0.360	0.357	0.351	0.354
1.5	0.293	0.263	0.224	0.241
1.6	0.232	0.185	0.147	0.164
1.7	0.183	0.130	0.105	0.116
1.8	0.141	0.093	0.079	0.085
1.9	0.115	0.067	0.063	0.064
2.0	0.090	0.050	0.050	0.050
2.2	0.060	0.029	0.035	0.034
2.4	0.041	0.020	0.026	0.024
2.6	0.029	0.016	0.025	0.020
2.8	0.021	0.015	0.021	0.017
3.0	0.015	0.014	0.015	0.015
3.2	0.010	0.013	0.010	0.012
3.4	0.007	0.011	0.007	0.009
3.6	0.005	0.009	0.005	0.007
3.8	0.004	0.006	0.004	0.005
4.0	0.002	0.003	0.004	0.004

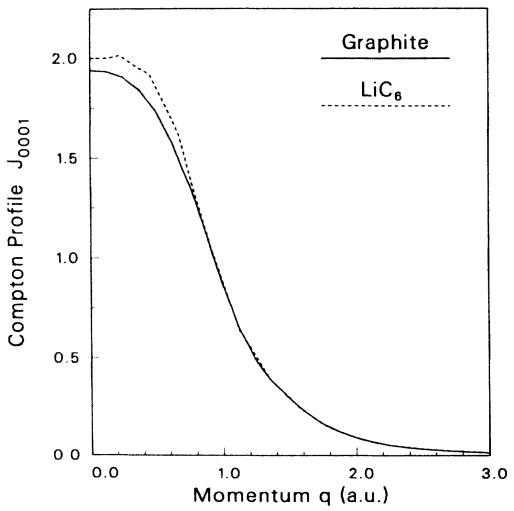

FIG. 2. Calculated Compton profiles for graphite (solid line) and LiC_6 (dashed line) along the [0001] direction. See text for the normalization.

[Fig. 3(a)], from the bonding π bands [Fig. 3(b)], and from the antibonding π^* (conduction) bands [Fig. 3(c)]. Graphite is a semimetal with about 0.01 eV overlap between the valence (π-bonding) and conduction (π-antibonding) bands. This detailed dispersion is beyond our calculational accuracy and we assume all the valence bands are occupied and conduction bands are empty in the evaluation of the Compton profile. Therefore, the graphite conduction bands do not appear in Fig. 3(c). Because of the symmetry of π and π^* orbitals, one should get zero amplitude at $q=0$ in Figs. 3(b) and 3(c).

The profiles of graphite and LiC_6 from the valence bands are very similar [Figs. 3(a) and 3(b)], except that for the LiC_6 case the profile amplitude increases slightly at small momenta and decreases at large momenta. This change in the momentum-space electron distribution corresponds to a slight delocalization in the real-space charge density which comes from the polarization effect of the lithium intercalant. This is more perceivable in Fig. 3(b) than in Fig. 3(a), because π orbitals have charge density located between layers and are more strongly affected upon intercalation.

The profile from the conduction bands of LiC_6 has some interesting characteristic features, as shown in Fig. 3(c). Periodic minima appear at 0, G_3, $2G_3$, . . . , where G_3 is the basic reciprocal-lattice vector along the [0001] direction with length 0.897 a.u. This behavior is related to the structure of the Fermi surfaces in LiC_6 where the Fermi level passes two conduction π bands to accommodate the extra electron.[5] As can be seen in Eq. (1), $J(q,\hat{e})$ is strongly dependent on the cross-sectional areas of the Fermi surface. In Fig. 4, the cross sections of the Fermi surfaces at $k_z=0$, 0.25, and 0.5 (in units of G_3) are shown. The cross sections of these two conduction bands are found to increase with k_z. The change is especially significant for the second conduction band. In particular, the state at M ($k_z=0$) is not occupied, but that at L ($k_z=0.5G_3$) is occupied. If one considers the momentum space cross sections in the periodic zone scheme, minima should be found at momenta with integral multiples of G_3. In addition to this phase volume effect, the structure of the wave functions should be included to get the detailed magnitude of the Compton profile [see Eq. (1)]. However, the main characteristics could be understood from the band structure of LiC_6. This point will be further discussed later in this section.

For a more detailed examination of the origin of the behavior in Fig. 3(c) and to isolate the intercalation effects, the Compton profile is also calculated for a hypothetical crystal C_6, which is obtained by removing the lithium atoms from LiC_6. The lattice constants and stacking sequence are the same as those of LiC_6, and one could shift the Fermi level to include the same number of electrons. As a result, the calculated Compton profile of the conduction bands is shown in Fig. 5(a), which is almost identical to the curve in Fig. 3(c). It is found that varying the energy of the Fermi level changes the curve considerably.

To illustrate the influence of the shapes of the volumes enclosed by the Fermi surface, a test is done by setting the plane-wave coefficients in Eq. (1) to a constant and recalculating the Compton profile. For the valence bands which are totally occupied, the profiles should be constant

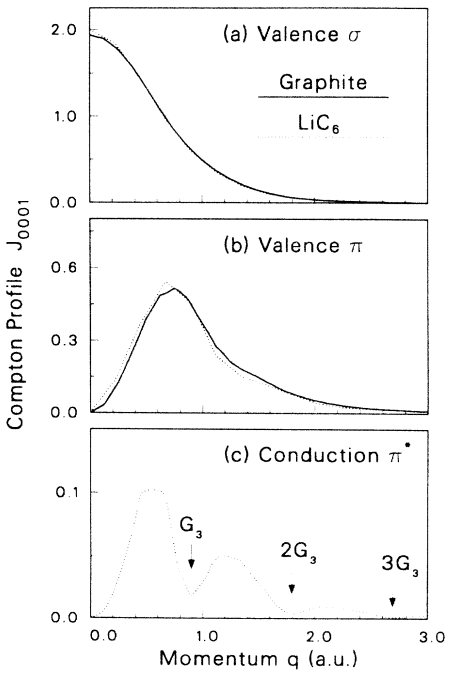

FIG. 3. Contributions from different energy bands to the Compton profiles of graphite (solid) and LiC_6 (dashed) in Fig. 1: (a) valence σ bands, (b) valence π (bonding) bands, and (c) conducting π^* (antibonding) bands.

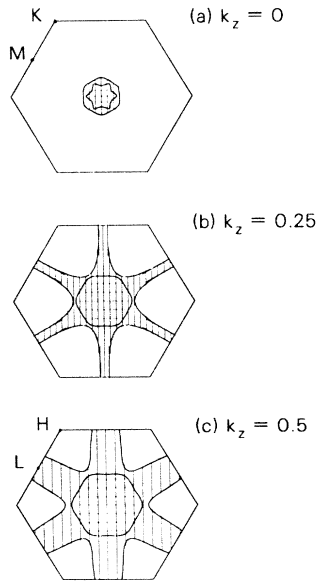

FIG. 4. Cross sections of the Fermi surfaces for two conduction bands in LiC_6 at $k_z=$ (a) 0.0, (b) 0.25, and (c) 0.5 (in units of G_3). The area belonging to the first (second) conduction band is shaded horizontally (vertically).

as a function of momentum. For the conduction bands, the result is proportional to the cross sections of occupied states in momentum space [as shown in Fig. 5(b)], and is periodic if all of reciprocal-lattice vectors are taken into account. There are distinct minima at 0, G_3, $2G_3$, etc. in Fig. 5(b). Because the symmetry of π orbitals is not included, the amplitude does not go to zero at $q=0$. Including the coefficients of actual wave functions is equivalent to adding an envelope function with π symmetry to the curve of Fig. 5(b). It is expected that this envelope function is similar to the profile of the valence π bands in Fig. 3(b) and goes to zero at both $q=0$ and $q=\infty$.

The similarity in the conduction-band profiles of C_6 and LiC_6 [Figs. 3(c) and 5(a)] indicates that the gross shape of the conduction-band structure of LiC_6 below the Fermi level originates in C_6. It is interesting to notice that the number of electrons lithium donates decides the position of the Fermi level and thus the features of the Compton profile of the conduction bands. Also shown in Fig. 5(c) is the conduction-band profile for graphite obtained by raising the Fermi level to have the same number of electronic states occupied. This is what one would obtain if the rigid-band model is applied. The overall shape is quite different from the LiC_6 and C_6 profiles in Figs. 3(c) and 5(a). Since the stacking sequence changes from $AAAA\cdots$ in C_6 to $ABAB\cdots$ in graphite, this induces a difference in the interlayer interaction which affects the detailed dispersions of the conduction bands and therefore the occupied states have a different momentum distribution.

So far our discussion has been focused on the results for the [0001] direction which is along the c axis and has the highest symmetry. Results along other directions are consistent with those discussed above for the [0001] direction, but the characteristic features of the conduction bands are not as apparent because of the inevitable overlapping and mixing when a less symmetric direction is considered.

B. Comparisons with experiment

The Compton profiles of graphite have been measured by several groups using photons in different energy ranges.[18–23] Since the samples of graphite are HOPG, measurable profiles are along the c-axis [0001] direction and the average obtained over xy plane. Two recent experimental results by Loupias *et al.*[21] and Vasudevan *et al.*[22] are compared with our calculated profiles in Fig. 6 along and perpendicular to the [0001] direction, respectively. The former experiment was performed using monochromatized 12.86-keV x rays from the Laboratoire pour l'utilisation du Rayonnement Elechromagnétique DCI synchrotron radiation beam and therefore obtained Compton profiles with a high resolution (0.15 a.u.). The latter used 412-keV γ rays from a ^{198}Au source and had a resolution of 0.4 a.u. These resolution functions are included in the calculated profile when comparisons are made. In Fig. 6(b), the contribution of carbon core electrons is calculated in the local-density-functional scheme

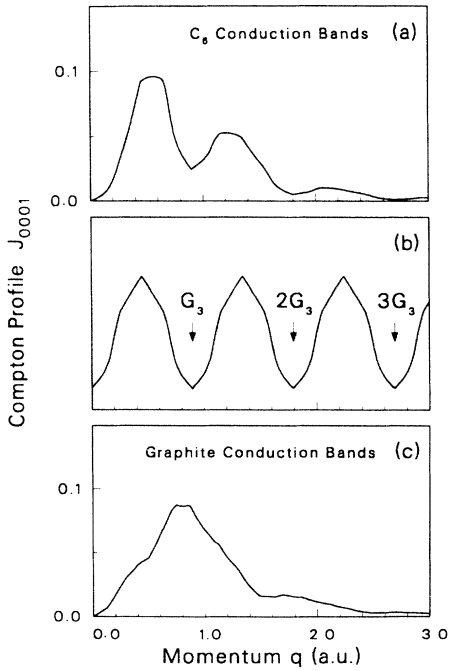

FIG. 5. (a) Calculated Compton profile for the conduction bands of C_6 along the [0001] direction. (b) Same as (a), except that the plane wave coefficients in Eq. (1) are taken to be constant (see text). (c) Calculated Compton profile for the conduction bands of graphite along the [0001] direction. In (a) and (c), the Fermi energy is raised to accommodate the additional $\frac{1}{6}$ electrons per carbon atom.

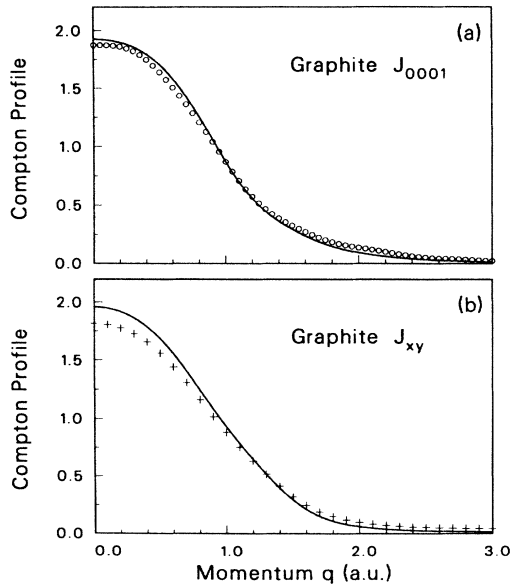

FIG. 6. Comparison of the Compton profile of graphite between the present calculation (solid line) and experimental results (a) along the [0001] direction (Ref. 21, circles) and (b) averaged over xy plane (Ref. 22, crosses). The appropriate experimental resolution functions have been used for the calculated results in the comparisons.

and is subtracted from the experimental results of Ref. 22. Since the oscillations of the valence wave functions near the core are left out in the pseudopotential approximation, we expect the calculated profiles to have a slightly smaller amplitude at large momenta and a larger amplitude at small momenta to maintain normalization. However, the overall agreement is very good.

To avoid systematic errors inherent in both the experiment and calculation,[30,31] it is more appropriate to compare the profile anisotropy. Moreover, the small magnitude of the profile anisotropy (for graphite it is less than 3% of the central peak in Fig. 2) demands high precision both in the experiment and calculation. The comparison in the profile anisotropy between theory and experiment is shown in Fig. 7. It is found that the agreement with both experiments are excellent and better than results from previous theoretical calculations,[20] where the disagreement could be 100% if the interlayer interaction is not accurately included. The remaining discrepancies in Fig. 7 might come from the use of the impulse approximation in this highly anisotropic material.

The Compton profiles of LiC_6 along the same two directions have also been measured by Loupias *et al.*[21] Comparisons with the theoretical results along the [0001] direction and the profile anisotropy are shown in Figs. 8(a) and 8(b), respectively. The agreement is similar in quality to that in graphite [Figs. 6(a) and 7(a)].

When the difference profile between LiC_6 and graphite is plotted, the intercalation effect can clearly been seen. Shown in Fig. 9 are both the calculated and measured difference profiles along the [0001] direction and averaged over xy plane. One can associate the features of the [0001] difference profile in Fig. 9(a) with different contributions in Fig. 3: the nonzero amplitude at $q=0$ comes from the polarization of the valence σ bands [Fig. 3(a)];

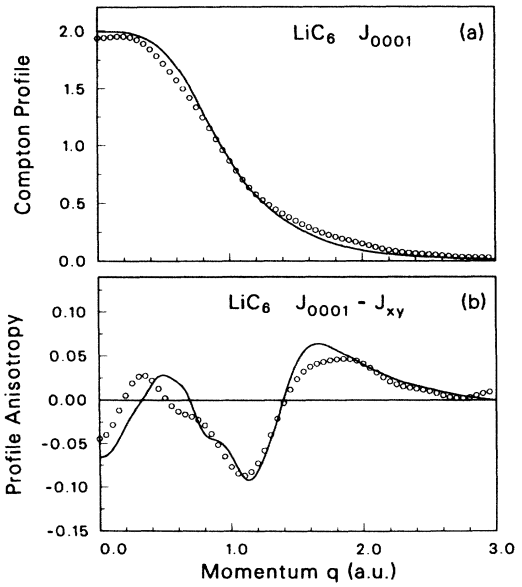

FIG. 8. Comparison of the Compton profile of LiC_6 between the present calculation (solid line) and experimental results (circles) in Ref. 21: (a) the [0001] profile, and (b) the profile anisotropy. The appropriate experimental resolution function has been used for the calculated results in the comparison.

the characteristic shapes of the conduction-band contribution of LiC_6 [Fig. 3(c)] are still visible and account for the drop at momenta near 0.9 a.u. These main features are observed in the experimental difference profile. On the other hand, these results are qualitatively different if a rigid-band model is assumed in Fig. 5(c). Good agreement between the calculation and experiment is also found for the xy profile in Fig. 9(b).

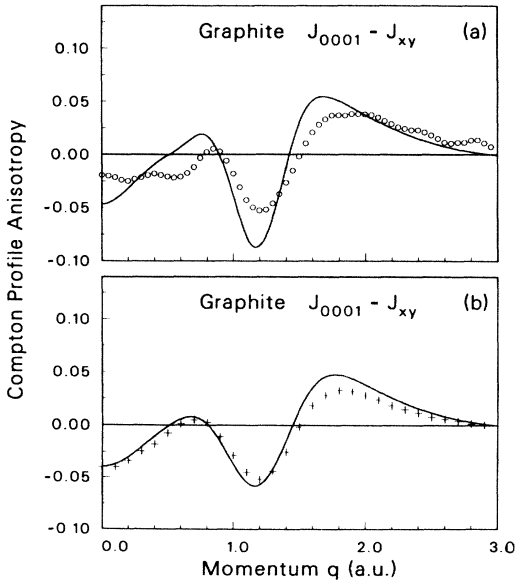

FIG. 7. Comparison of the Compton profile anisotropy in graphite between the present calculation (solid line) and experimental results in (a) Ref. 21 (circles) and (b) Ref. 22 (crosses).

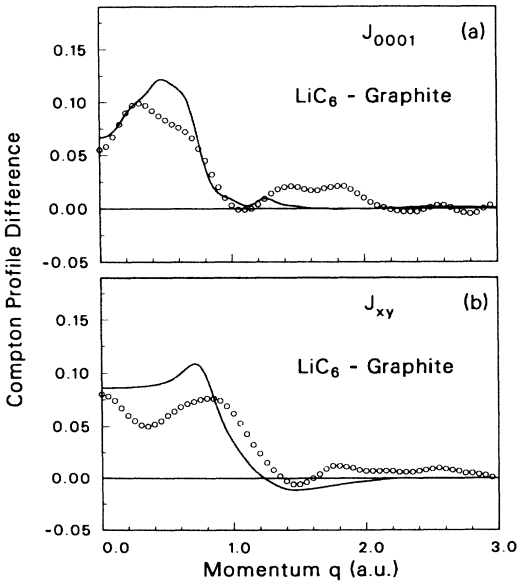

FIG. 9. Difference between the profiles of LiC_6 and graphite: (a) along the [0001] direction and (b) averaged over xy plane. The solid lines are the present result. Circles stand for experimental data in Ref. 21.

There are other experimental techniques (for example, positron annihilation and electron scattering) that probe the electron momentum distribution. Some measurements have been performed for graphite.[32–34] In the case of positron annihilation,[32,33] the cross sections for σ and π electrons are quite different; therefore it is difficult to make comparisons between the present results and the positron annihilation spectra. It is also possible to measure the Compton profiles of graphite by means of electron scattering, but at this time the measurements are restricted to scattering directions along the hexagonal plane.[34] This new technique is being refined to get higher resolution and intensity.[35]

IV. CONCLUSION

In summary, we have calculated the Compton profiles for graphite and LiC_6 along several symmetry directions within the impulse approximation. The wave functions employed are obtained from previous self-consistent pseudopotential calculations using the local-density-functional scheme.[5] The overall calculated results are in good agreement with experiment. In particular, the agreement in the profile anisotropy is excellent. This suggests that the ground-state wave functions obtained from this theoretical approach can be viewed as highly accurate.

The Compton profiles provide a new point of view to examine the effects of intercalation on momentum space properties. A polarization effect resulting from the lithium intercalant is found when the [0001] profiles of valence bands are compared between LiC_6 and graphite. On the other hand, the profile of LiC_6 conduction bands along the same direction shows a certain characteristic oscillation related to the band structure of the empty lattice C_6 and to the Fermi-level position. These two effects appear in the total difference profile of the [0001] direction between LiC_6 and graphite and result from the intercalation and the consequent stacking change. A comparison with the profile of the graphite conduction bands shows that the rigid-band model does not explain the detailed structure of the electron momentum distributions.

ACKNOWLEDGMENTS

We would like to thank Professor N. A. W. Holzwarth for providing the calculated wave functions, Dr. G. Loupias and Dr. J. Chomilier for the use of their data and for helpful discussions, and Dr. R. Holt for sending us experimental data prior to publication. This work is supported by National Science Foundation Grant No. DMR8319024 and by the Director, Office of Energy Research, Office of Basic Energy Sciences, Material Sciences Division of the U.S. Department of Energy under Contract No. DE-AC03-76SF00098.

[1]For a review of graphite, see B. T. Kelly, *Physics of Graphite* (Applied Science, London, 1981).
[2]For a review of graphite intercalation compounds, see M. S. Dresselhaus and G. Dresselhaus, Adv. Phys. **30**, 139 (1981).
[3]N. A. W. Holzwarth, S. Rabii, and L. A. Girifalco, Phys. Rev. B **18**, 5190 (1978).
[4]R. V. Kasowski, Phys. Rev. B **25**, 4189 (1982).
[5]N. A. W. Holzwarth, S. G. Louie, and S. Rabii, Phys. Rev. B **28**, 1013 (1983).
[6]P. Oelhafen, P. Pfluger, E. Hauser, and H.-J. Güntherodt, Phys. Rev. Lett. **44**, 197 (1980).
[7]W. Eberhardt, I. T. McGovern, E. W. Plummer, and J. E. Fisher, Phys. Rev. Lett. **44**, 200 (1980).
[8]U. M. Gubler, P. Oelhafen, and H.-J. Güntherodt, Solid State Commun. **44**, 1621 (1982).
[9]G. K. Wertheim, P. M. Th. M. Van Attekum, and S. Basu, Solid State Commun. **33**, 1127 (1980).
[10]C. F. Hague, C. Indlekofer, U. M. Gubler, P. Oelhafen, H.-J. Gütherodt, and J. Schmidt-May, Solid State Commun. **48**, 1 (1983).
[11]C. Marinos, S. Plesko, J. Jonas, J. Conard, and D. Guérard, Solid State Commun. **47**, 645 (1983).
[12]J. Conard, H. Estrade, P. Lauginie, H. Fuzellier, G. Furdin, and R. Vasse, Physica **99B**, 521 (1980).
[13]N. A. W. Holzwarth, S. G. Louie, and S. Rabii, Phys. Rev. B **26**, 5382 (1982).
[14]P. M. Platzman and N. Tzoar, Phys. Rev. **139**, A410 (1965); P. Eisenberger and P. M. Platzman, Phys. Rev. A **2**, 415 (1970).
[15]For a general reference, see *Compton Scattering*, edited by B. G. Williams (McGraw-Hill, New York, 1977).
[16]B. L. Hicks, Phys. Rev. **57**, 665 (1940).
[17]P. Eisenberger and W. C. Marra, Phys. Rev. Lett. **27**, 1413 (1971).
[18]M. Cooper and J. A. Leake, Philos. Mag. **5**, 1201 (1967).
[19]T. L. P. Paakari, Phys. Fenn. **9**, 185 (1974).
[20]W. A. Reed, P. Eisenberger, K. C. Pandey, and L. C. Snyder, Phys. Rev. B **10**, 1507 (1974).
[21]G. Loupias, J. Chomilier, and D. Guérard, J. Phys. Lett. (Paris) **45**, L301 (1984); G. Loupias, J. Chomilier, and D. Guérard, Solid State Commun. **55**, 299 (1985).
[22]S. Vasudevan, T. Rayment, B. G. Williams, and R. Holt, Proc. R. Soc. London, Ser. A **391**, 109 (1984).
[23]R. Tyk, J. Felsteiner, I. Gertner, and R. Moreh, Phys. Rev. B **32**, 2625 (1985).
[24]M. Y. Chou, S. G. Louie, M. L. Cohen, and N. A. W. Holzwarth, Phys. Rev. B **30**, 1062 (1984).
[25]G. Lehmann and M. Taut, Phys. Status Solidi B **54**, 469 (1972).
[26]M. L. Cohen, Phys. Scr. T **1**, 5 (1982).
[27]P. Hohenberg and W. Kohn, Phys. Rev. **136**, B864 (1964); W. Kohn and L. J. Sham, Phys. Rev. **140**, A1133 (1965).
[28]S. G. Louie, K. M. Ho, and M. L. Cohen, Phys. Rev. B **19**, 1774 (1979).
[29]R. C. Tatar and S. Rabii, Phys. Rev. B **25**, 4126 (1982), and references therein.

[30]M. Y. Chou, P. K. Lam, M. L. Cohen, G. Loupias, J. Chomilier, and J. Petiau, Phys. Rev. Lett. **59**, 1452 (1982); M. Y. Chou, P. K. Lam, and M. L. Cohen, Phys. Rev. B **28**, 1696 (1983).

[31]G. E. W. Bauer and J. R. Schneider, Solid State Commun. **47**, 673 (1983); Phys. Rev. B **31**, 681 (1985).

[32]S. Berko, R. E. Kelley, and J. S. Plaskett, Phys. Rev. **106**, 824 (1957).

[33]E. Cartier, F. Heinrich, P. Pfluger, and H.-J. Güntherodt, Solid State Commun. **33**, 1127 (1980).

[34]B. G. Williams and A. J. Bourdillon, J. Phys. C **15**, 6881 (1982).

[35]B. G. Williams, T. G. Sparrow, and R. F. Egerton, Proc. R. Soc. London, Ser. A **393**, 409 (1984).